



## Variability in the Cretan Sea (Eastern Mediterranean) from six years' glider observations (2017- 2023)

Evi Bourma<sup>1</sup>, Dionysios Ballas<sup>1</sup>, Gerasimi Anastasopoulou<sup>1</sup>, Natalia Stamatakis<sup>2</sup>, Spyros Velanas<sup>1</sup>, Manos Pettas<sup>2</sup>, George Petihakis<sup>2</sup> and Leonidas Perivoliotis<sup>1</sup>

5 <sup>1</sup>Institute of Oceanography, Hellenic Centre for Marine Research, GR-190 13 Anavyssos, Greece

<sup>2</sup>Institute of Oceanography, Hellenic Centre for Marine Research, GR-71 003 Heraklion, Greece

*Correspondence to:* Evi Bourma (evibourma@hcmr.gr)

**Abstract.** The Cretan Sea is an intermediate and occasionally deep water formation area within the Eastern Mediterranean that accumulates and transforms water masses from the adjacent Aegean, Levantine and Ionian Seas. Six years of glider 10 observations (2017–2023) in the Cretan Sea were analysed to study the properties, variability and dynamics of the water masses during the study period. The analysis revealed progressive warming and salinification of the intermediate and deep layers. The mean temperature increased by around 0.05–0.07 °C per year, and the salinity by approximately 0.02 per year. Furthermore, comparisons with climatological data from 2000 to 2015 show temperature departures of +0.4 to 0.6 °C in the upper 400 m and salinity increases of up to +0.3 at the surface. Both of these values decline with depth, highlighting the intensified warming 15 and increased salinity near the surface and in the upper intermediate layers. Additionally, the analysis of salinity and temperature datasets revealed the formation of intermediate water annually, except in winter 2022 when an intense mixing event occurred in the Cretan Sea triggered by exceptionally cold atmospheric conditions. The mixed layer, as captured by the glider, extended below 600 m inside the Cretan basin. These newly formed waters almost reached the deep layers, significantly modifying the properties of the intermediate and deep waters, although full deep convection was not reached. The observed 20 downward displacement of the TMW core below 1000 m is associated with the strong convective event as well as with the redistribution of the heat and salt in the intermediate and deep layers. These findings emphasize the importance of sustained, high-resolution observations in capturing both gradual trends and extreme events, and in improving our understanding of the evolving thermohaline circulation of the Eastern Mediterranean.

### 1 Introduction

25 The Cretan Sea is located in the southern Aegean region expanding north of the island of Crete. It constitutes a key contributor to the thermohaline circulation of the Eastern Mediterranean, representing one of the major dense water formation sites, along with the Levantine, Adriatic and north Aegean Seas. The occurrence of the Eastern Mediterranean Transient (EMT) in the early 1990s, highlighted the significance and role of the Cretan Sea within the Eastern Mediterranean; the wider area of Aegean Sea has been recognized as a major contributor to the renewal of deep and bottom waters of the Eastern Mediterranean (Pinardi 30 et al., 2023). It is considered to act as a heat and salt repository that accumulates water masses originating from various Aegean



Sea sub-basins (Theocharis et al., 1993, 1999), as well as an active intermediate and occasionally deep water mass source (Velaoras et al., 2014).

The Cretan basin has a mean depth of roughly 1000 m, with two eastern depressions reaching 2200–2500 m (Theocharis et al., 1999). It communicates with the EMed (Ionian and Levantine Seas), exchanging water masses, through the Cretan Straits, 35 Kassos, Karpathos and Rhodes straits at the east, while at the west, Antikythira, Kythira and Elafonisos straits. Out of the Cretan Straits, south of Crete the seabed deepens sharply to depths of 3000–4000 m toward the Hellenic Trench (Velaoras et al., 2014) (Fig.1).

The surface and subsurface layers are strongly affected by the warm, saline Levantine Surface Water (LSW) entering mainly from the east, while fresher modified Atlantic Water (AW) enters occasionally through the western straits. Waters from the 40 north are also reaching the Cretan area; the Brackish Black Sea Water (BSW) entering the Aegean through the Dardanelles straits, influences the northern Aegean and, after mixing over the Cyclades Plateau, reaches the western Cretan Sea with higher salinity (Velaoras et al., 2019). At intermediate depths, the basin is occupied by Levantine Intermediate Water (LIW), while winter convection periodically forms Cretan Intermediate Water (CIW), which seems to be rather denser than LIW settling a bit deeper, presenting though interannual variability (Velaoras et al., 2019). The deep and bottom layers are filled with Cretan 45 Deep Water (CDW), high density waters which accumulated at the bottom layers during the EMT event (Velaoras et al., 2019). Between the intermediate and deep layers lies the Transitional Mediterranean Water (TMW), a relatively fresh, oxygen-poor but nutrient-rich mass whose depth varies over time.

The extreme EMT event was well documented throughout its three phases of evolution: the EMT onset phase (1987–1991), the EMT peak phase (1992–1995) and the EMT relaxation phase (until the early 2000s) (Roether et al., 1996; 2007; Klein et 50 al., 1999; Theocharis et al., 1999a; 1999b; 2002; Gertman et al., 1994; Kontoyiannis et al., 1999; Sur et al., 1992). This abrupt event triggered fresh interest and further research in the Cretan Sea, and improved understanding of the mechanisms driving the circulation in the Eastern Mediterranean. Several conceptual frameworks have been proposed. Gačić et al. (2011) suggested that the Northern Ionian Gyre (NIG) circulation influences the hydrology of the Eastern Mediterranean through the Adriatic–Ionian Bimodal Oscillating System (BiOS), when cyclonic and anticyclonic modes alternately enhance and modulate deep- 55 water formation in the Adriatic or the Aegean/Levantine Seas. In contrast, Theocharis et al. (2014) proposed the “thermohaline pump” mechanism based on an anti-correlated, quasi-decadal oscillation between the Adriatic and Aegean Seas acting as competitive dense water formation sources. According to this view, shifts in the AW pathway and changes in salinity precondition each basin for alternating dense water formation (DWF) phases. Both Krokos et al. (2014) and Velaoras et al. (2014) emphasized that a salinity preconditioning phase is essential for dense water formation, consistent with the 60 “thermohaline pump” mechanism proposed by Theocharis et al. (2014). Their analyses showed that, during the second half of the 2000s, the Cretan Sea exported intermediate water masses denser than typical LIW/CIW but not dense enough to reach the deep Eastern Mediterranean layers. This outflowing water mass was termed dense Cretan Intermediate Water (dCIW), and the authors identified these occurrences as “EMT-like” events, indicating conditions similar to those during the Eastern Mediterranean Transient. Furthermore, Velaoras et al. (2015) linked TMW appearance in the Cretan basin to water mass



65 exchanges driven by DWF in the Aegean Sea, where the export of dense Aegean waters through the Cretan Straits is compensated by TMW inflow. Consequently, TMW acts as a tracer for Aegean DWF, with the depth of intrusion indicating the strength of the event. TMW also transports nutrients to the oligotrophic Cretan Sea, thereby extending its impact on local ecological processes.

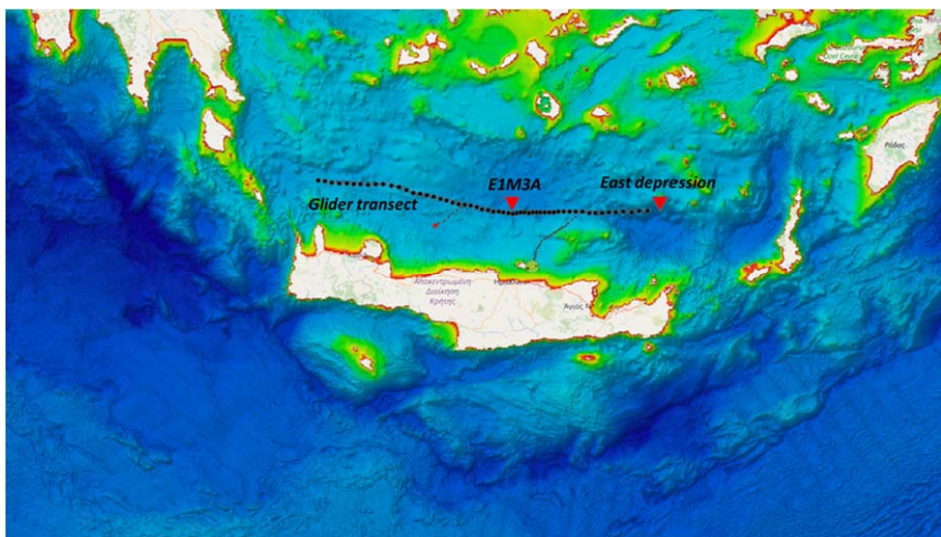
Overall, the Cretan Sea is a dynamic region having its specific role in the eastern Mediterranean due to its thermohaline 70 interplay with the adjacent North Aegean, Ionian and Levantine Seas. The seasonal and interannual variability driven by combined effects -atmospheric forcing, oceanic circulation, formation and transformation processes - is a structural component of the mechanism governing the exchanges and interplay with the neighbouring basins. In addition, these processes are inevitably affected by climatic trends, making sustained observations crucial for assessing the long-term impact of climate change and interpreting the evolving dynamics of the Eastern Mediterranean circulation.

75 In this context, the endurance line in the Cretan Sea (Fig. 2) has been established and is operating since late 2017, providing high-resolution observations and enabling sustained monitoring of the basins 's hydrographic structure and its variability. This endurance line marks the first operational deployment of the glider component of the POSEIDON system ([www.poseidon.hcmr.gr](http://www.poseidon.hcmr.gr)), an ocean observatory research infrastructure dedicated to monitoring and forecasting the marine environment of the Eastern Mediterranean (Petihakis et al., 2018). The POSEIDON system and its glider component also form 80 part of the National Marine Research Infrastructure HIMIOFoTS. (Bourma et al., 2022).

The scope of this study is to provide a comprehensive description of the oceanographic state and the hydrography in the Cretan Sea, analysing salinity and temperature data collected during the 6 years of glider observations between 2017 and 2023, as well as the temporal evolution of the dynamics governing this key subsystem within the Eastern Mediterranean circulation. The paper is organized as follows. Sect. 2 describes the glider dataset and methods used. Sect. 3 presents the seasonal 85 characteristics and the hydrographic structure in the Cretan Sea and highlights extreme events recorded during the study period. Sect. 4 examines the interannual variability of the surface, intermediate, and deep layers, and presents six-year trends in temperature and salinity for the intermediate and deep waters. Deviations from the climatological properties are also investigated in this section, endeavouring to quantify changes in relation to the Cretan Sea's past state. The analysis is complemented by an examination of the temporal evolution the TMW mass residing in the Cretan Basin, as it is strongly linked 90 to convection processes in the region. Finally, Sect.5 summarizes the main findings and concludes.



Figure 1: Bathymetric map of the Eastern Mediterranean Sea, the Cretan Sea, straits and adjacent basins from EMODnet Bathymetry World Base Layer (EBWBL), (EMODnet Bathymetry Consortium, 2016).



95 Figure 2: The glider transect north of Crete is shown by the black dots marking its east-to-west extent. The locations of the CTD casts used in this study are also indicated, with red triangles marking the E1M3A POSEIDON buoy and the eastern depression of the Cretan Basin (2090 m). The glider transect was visualized on the EMODnet bathymetry map layer (EMODnet Bathymetry Consortium, 2016) through ‘GLIMPSE’, the ALSEAMAR mission management tool.



## 100 2 Glider observations in the Cretan Sea

Since 2017, HCMR has conducted repeated missions in the Cretan Sea using ALSEAMAR SeaExplorer gliders. During each mission, the glider performs continuous profiling along a transect approximately parallel to the northern coast of Crete, with a total length of about 220 km (Fig. 2). Mission durations range from 30 to 45 days, during which the glider typically completes the transect two to three times. The sampling depth varies according to the bathymetry and the glider maximum operational 105 depth to 700 m or 1000 m. Its horizontal velocity (SOG - speed over ground) fluctuates between 0.15 and 0.4 m/s (depending on the direction and the magnitude of the sea currents) while its vertical velocity has values between 0.1 and 0.2 m/s. Payload includes a CTD (conductivity, temperature, depth) and a dissolved oxygen sensor (GPCTD + DO, Sea-Bird Electronics). Data quality control includes pre- and post-calibration checks of the sensors, while validation is performed through comparisons with reference CTD casts acquired during deployment and recovery of the glider. The measured variables include pressure, 110 temperature, conductivity and dissolved oxygen. Glider data were processed with the EGO data processing chain to generate EGO-compliant NetCDF files (EGO Gliders Data Management Team, 2025a), which include standard automatic and manual quality control procedures (EGO Gliders Data Management Team, 2025b). In addition, all sensors mounted on the gliders are maintained in accordance with manufacturer specifications.



115 **Figure 3: Distribution of glider missions by year (2017–2023) and season (top panel). The operational depth of each mission—either 700 m or 1000 m—is shown below.**



Conversions using the Thermodynamic Equation of Seawater (TEOS-10) functions were applied to obtain potential temperature (hereafter temperature) and practical salinity (hereafter salinity) (IOC, SCOR, and IAPSO, 2010). The vertical profiles were then interpolated onto a uniform depth grid of 1 m and a horizontal resolution of 4 km along the glider track, in  
120 order to facilitate comparison and computation across missions. The mixed layer depth (MLD) was calculated directly from the raw SeaExplorer measurements (30 s sampling), prior to any interpolation, using a density-threshold criterion of 0.03 kg m<sup>-3</sup> relative to the density at 10 m depth (de Boyer Montégut et al., 2004).  
To provide a synoptic representation of the surface circulation, we used the European Seas Gridded L4 Sea Surface Heights and Derived Variables — Reprocessed Product from the Copernicus Marine Service (2024), which provides absolute dynamic  
125 topography and surface geostrophic velocities. Additional data used to complement our results are conductivity–temperature–depth (CTD) casts sampled with a shipborne probe in the locations depicted in Fig. 2 as well as the time series data recorded by the E1M3A fixed buoy in the depth levels of 250, 400, 600 and 1000 m. CTD data were collected using Seabird SBE 911+ CTD probes with a 24 Hz sampling rate and processed with the manufacturer's (Sea-Bird) software routines and interpolated to 1 dbar bins.  
130 Glider missions have been conducted since late 2017, but their occurrence has not been evenly distributed across seasons or months. Fig. 3 (top) presents the fourteen missions categorized by season and year. For the purpose of this study, we define the seasons as follows: winter (January–March), spring (April–June), summer (July–September), and autumn (October–December). Most missions were conducted during the winter and autumn months, while spring and summer are underrepresented. This imbalance reflects both operational constraints and scientific priorities. Winter and autumn missions  
135 are emphasized in order to capture the most dynamically active period of convection and water-mass transformation, whereas logistical limitations and the calmer summer conditions have resulted in fewer spring and summer deployments. This seasonal bias is considered in the analyses that follow.  
A further limitation arises from the variability in maximum dive depth across missions: while some glider deployments reached 1000 m (8 of 14 missions in total), others were restricted to 700 m (6 of 14 missions in total) as presented in Fig. 3, bottom.  
140 This uneven vertical coverage introduces gaps in the characterization of intermediate and deep water masses, particularly below 700 m. Furthermore, none of the glider profiles reached the seafloor due to glider operational limitations, leaving the deepest layers of the Cretan Basin unsampled. Therefore, interpretations of deep variability should be treated with caution, bearing in mind that the available observations do not capture the full vertical structure of the water column.

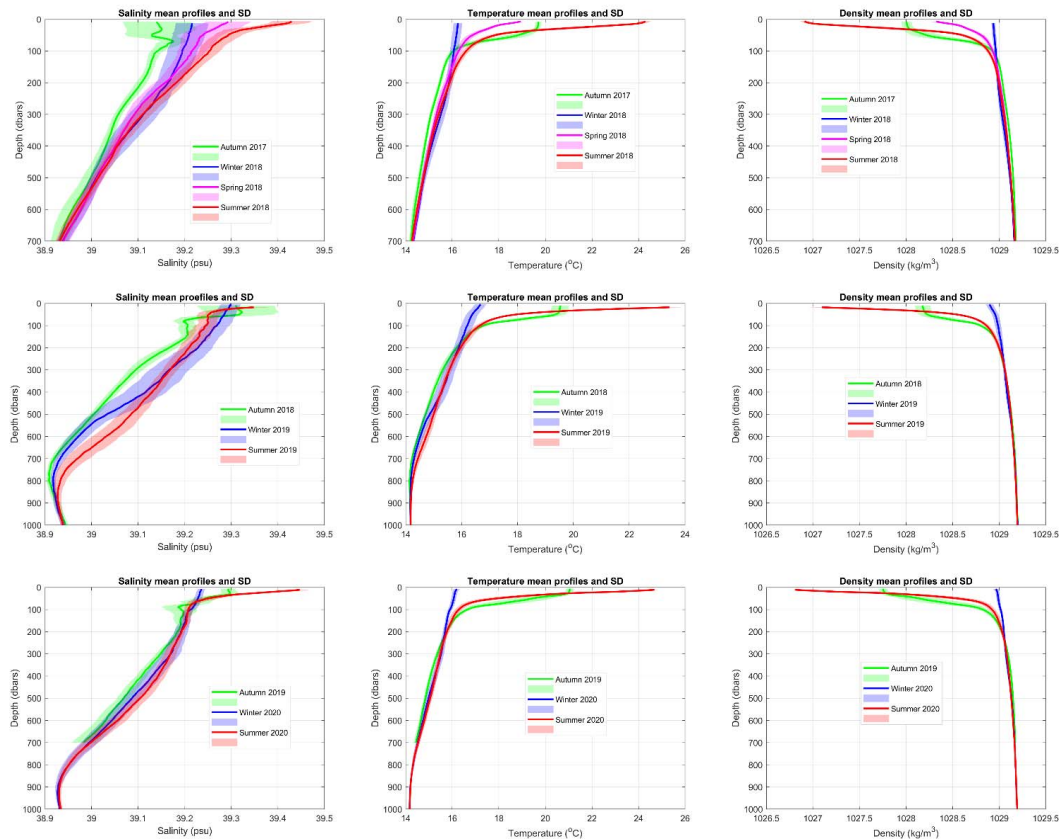
### 3 Seasonal variability and the oceanographic state during the study period

145 In this section, we describe the water masses and the oceanographic characteristics of the Cretan Sea during the study period from the perspective of the region's dominant seasonal cycle. In order to accomplish that, at first we examine the seasonal patterns derived from mean vertical profiles of key variables, then we describe the water masses and their properties using



seasonal T- S diagrams and vertical sections across the glider transect of salinity, temperature and density, together with the corresponding satellite-derived absolute dynamic topography fields.

150 The seasonal mean profiles of temperature, salinity, and potential density  $\sigma_0$  (hereafter density) along the west-east glider transect as presented in Fig. 4., reveal seasonal patterns characterized by strong surface stratification in summer, enhanced mixing and cooling in winter, and transitional spring and autumn stages that reflect the gradual adjustment of the water column. The seasonal mean profiles from the first three annual cycles, that are presented in Fig. 4, (autumn 2017–summer 2018, autumn 2018–summer 2019, and autumn 2019–summer 2020) are indicating nearly uniform temperature and density profiles during 155 winter, ranging from  $\sim 14.33 \text{ }^{\circ}\text{C} / 29.16 \text{ kg m}^{-3}$  near the maximum deployment depth to  $16.25 \text{ }^{\circ}\text{C} / 28.95 \text{ kg m}^{-3}$  at the surface. In spring, surface warming generates higher temperatures and lower densities in the upper  $\sim 100 \text{ m}$  ( $\sim 14.31 \text{ }^{\circ}\text{C} / 29.165 \text{ kg m}^{-3}$  near the maximum deployment depth to  $18.93 \text{ }^{\circ}\text{C} / 28.32 \text{ kg m}^{-3}$  at the surface), accompanied by the gradual formation of a pycnocline. Summer is marked by intensified surface heating and the strong establishment of the pycnocline ( $\sim 14.27 \text{ }^{\circ}\text{C} / 29.17 \text{ kg m}^{-3}$  near the maximum deployment depth to  $19.69 \text{ }^{\circ}\text{C} / 26.91 \text{ kg m}^{-3}$  at the surface), while in autumn cooling and convection 160 progressively erode this stratification ( $\sim 14.23 \text{ }^{\circ}\text{C} / 29.18 \text{ kg m}^{-3}$  near the maximum deployment depth to  $24.3 \text{ }^{\circ}\text{C} / 28 \text{ kg m}^{-3}$  at the surface). Reported values refer to the first more complete seasonal cycle represented in Fig. 4, 1st row. The above mentioned seasonal cycles are not evident in the mean salinity profiles, as the observed variability mainly reflects 165 the continuous exchanges between the Cretan Sea and the surrounding Eastern Mediterranean and Northern Aegean Sea. These exchanges introduce water masses with diverse salinity signatures influenced by processes occurring on non-seasonal or intermittent timescales. A typical example can be the inflow of fresher modified AW, partially modulated by the NIG as it alternates between cyclonic and anticyclonic circulation regimes.

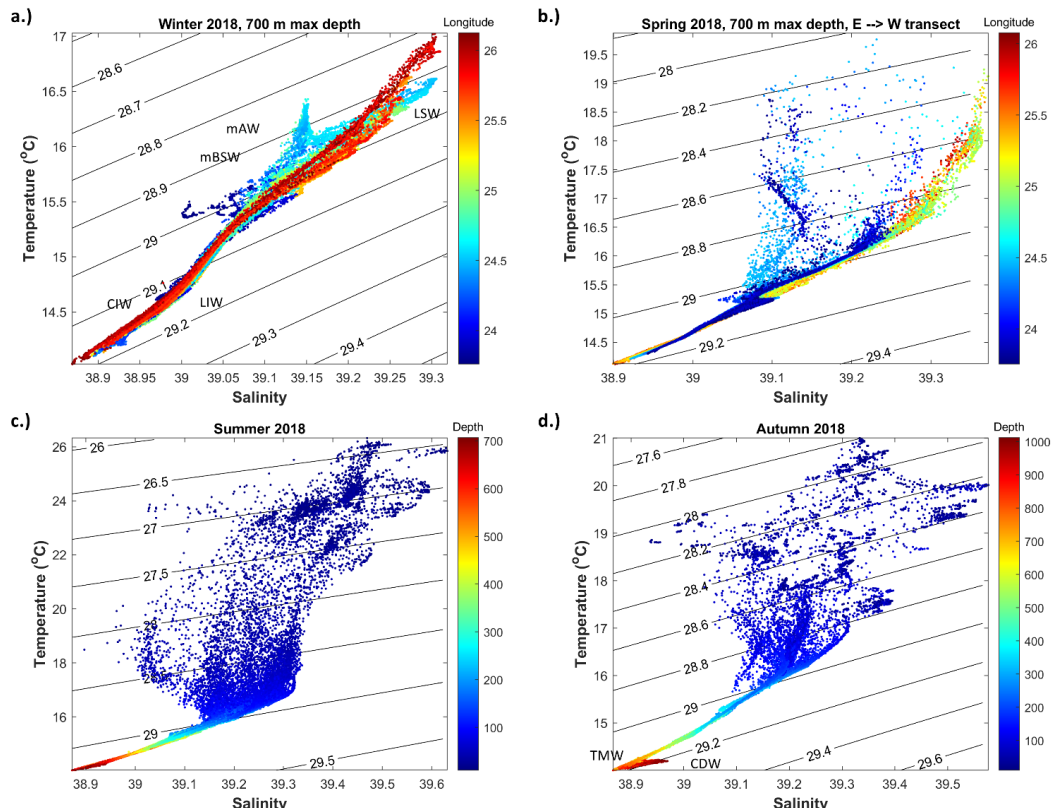


170 **Figure 4: Mean profiles of the salinity, temperature, density and standard deviations – SD (shade) – calculated for each transect** (eastern to western edge or vice versa). Successive seasonal mean profiles are presented yearly: Autumn 2017 – Winter 2018 – Spring 2018 - Summer 2018 (1st row), Autumn 2018 – Winter 2019 - Summer 2019 (2nd row), Autumn 2019 – Winter 2020 – Summer 2020 (3rd row).

175 The T–S diagrams for each season presented in Fig. 5 illustrate the hydrographic structure of the Cretan Sea. In winter and spring 2018, the diagrams are colored by latitude to show how water-mass properties vary spatially along the transect (Fig. 5a and 5b). In summer and autumn 2018, they are colored by depth to emphasize the vertical density structure of the water column (Fig. 5c and 5d). Cretan Surface Waters (CSW) are typically influenced by LSW and fresher modified AW/BSW inflows producing evident spatial gradients in surface temperature and salinity. At intermediate depths, CIW and LIW coexist within overlapping layers displaying similar thermohaline signatures. As reported by Velaoras et al. (2019), CIW is generally denser than LIW, although its properties vary interannually depending on the depth and strength of winter convection. TMW occupies depths below ~600 m during autumn 2018, forming the characteristic low-salinity “hump” visible in Fig. 5d, while the older



CDW resides beneath it. The deepest part of the CDW, however, is not fully captured due to the 1000 m depth limitation of the glider.



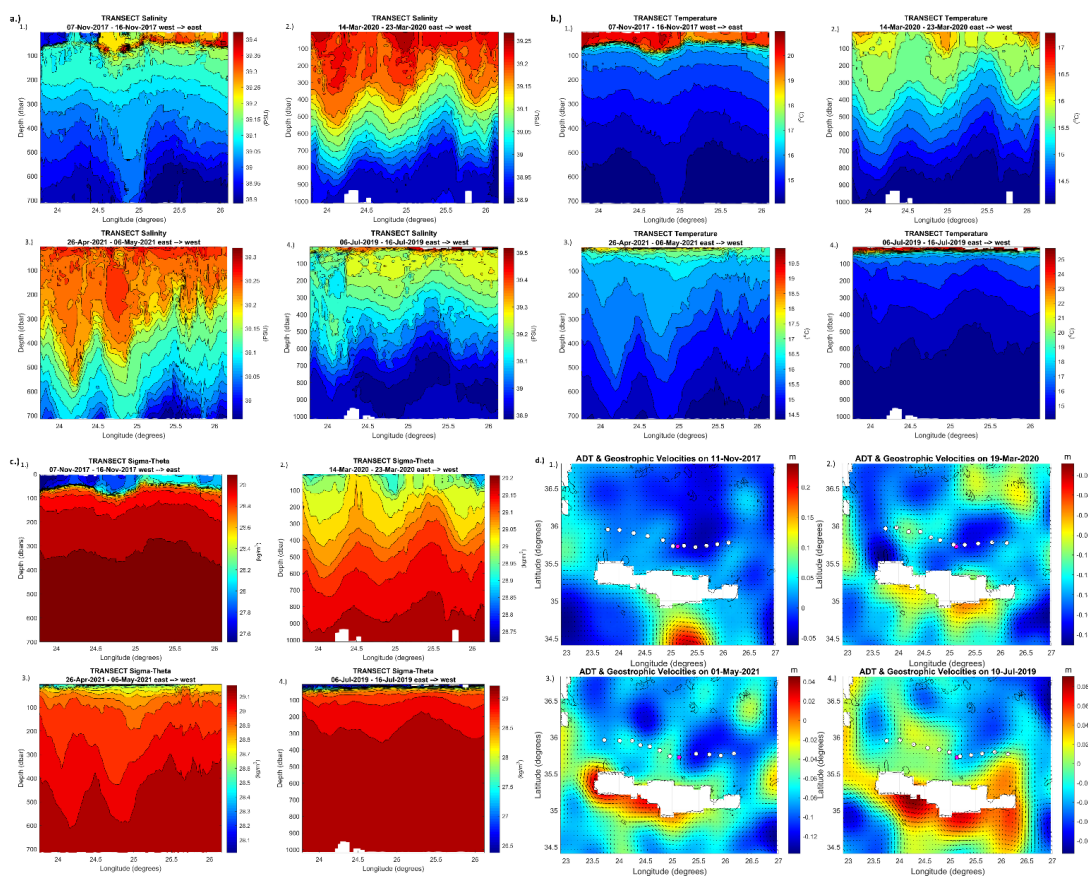
185 **Figure 5: T-S seasonal diagrams:** Winter 2018 (a) and spring 2018 (b) are coloured by latitude to highlight spatial distribution, while summer 2018 (c) and autumn 2018 (d) are coloured by depth to reveal vertical structure.

In Figure 6 (a, b, c), the transect diagrams of salinity, temperature, and density illustrate how these properties vary horizontally across the Cretan Sea—from west to east—and vertically from the surface down to 700 or 1000 m, depending on each glider's operational depth. When considered collectively across all missions, these transects reveal distinct and recurring seasonal 190 patterns as well as a strong dependence on the mesoscale eddies that dominate the area. These dynamics are demonstrated in Figure 6 which depicts some representative transects for each season: autumn 2017 (07–16 November), winter 2020 (14–23 March), spring 2021 (26 April–06 May), and summer 2019 (06–16 July). Each transect is paired with the corresponding horizontal Absolute Dynamic Topography (ADT) field for the same period (11 November 2017, 19 March 2020, 01 May 2021, and 10 July 2019), providing a synoptic view of the circulation that shapes the observed vertical and horizontal structures.



195 The autumn 2017 salinity transect (Fig. 6a) captures fresher waters on the west and more saline waters on the east in the upper ~100 m, meeting within an anticyclonic structure centred between 24.5°E and 25°E (Fig. 6d). The doming of isohalines observed down to ~700 m depth is indicative of downwelling (Fig. 6a (1)) and further reflects the influence of this anticyclone, as confirmed by the ADT fields and associated geostrophic velocity vectors (Fig. 6d (1)). The low salinity signature of TMW is also evident in the deep layers of the salinity transects (Fig. 6a), particularly in missions that reached 1000 m depth.

200 The temperature transects in Fig. 6b present intense surface warming and stratification in summer, followed by cooling and progressive deepening of the mixed layer toward winter. Density transects reflect the combined effects of temperature and salinity, showing a well-defined seasonal progression: deep winter mixing, pycnocline formation in spring, strong summer stratification, and partial erosion of density gradients during autumn.



205

**Figure 6: a.) Salinity along the transect during autumn (07 to 16 November 2017), winter (14 to 23 March 2020), spring (26 April to 06 May 2021) and summer (06 to 16 July 2019). b.) Temperature transects diagrams for the same missions and duration (autumn**



2017, winter 2020, spring 2021 and summer 2019). c.) Sigma – theta along the transect during the corresponding days for autumn  
210 2017, winter 2020, spring 2021 and summer 2019 and d.) Fields of Absolute Dynamic Topography with superimposed geostrophic  
velocity vectors (Copernicus marine service, 2024) for the respective dates to the presented seasonal missions, that is: 11 November  
2017, 19 March 2020, 01 May 2021 and 10 July 2019. White dots represent the glider transect and the red dot is the E1M3A position.

### 3.1 Water mass formation

Convective mixing of the water column during winter and early spring leads to the development of an extended mixed layer, marking the occurrence of intermediate and occasionally deep-water formation events throughout these periods as extensively  
215 reported in Velaoras et al., (2014). During the six years of the glider observations, maximum MLD values did not exceed ~30 m in summer, ~120 m in autumn, and ~360 m in winter, with the notable exception of winter 2022, when it reached a depth of approximately 625 m as denoted in Table 1, where the estimated values of maximum MLD are presented for all the missions, and the Fig. 7b which presents the temporal evolution of these maximum values. As shown, intermediate water formation is observed every winter, with the highlight of winter 2022, when the glider revealed MLD exceeding 600 m. According to the  
220 State of the Climate 2022 report by the American Meteorological Society, temperatures in March 2022 were below normal as cold air from Russia advanced toward the eastern and central Mediterranean. Greece reported a monthly anomaly of  $-3.0^{\circ}\text{C}$  — the third coldest March on record — mainly due to a cold wave from 9 to 16 March.

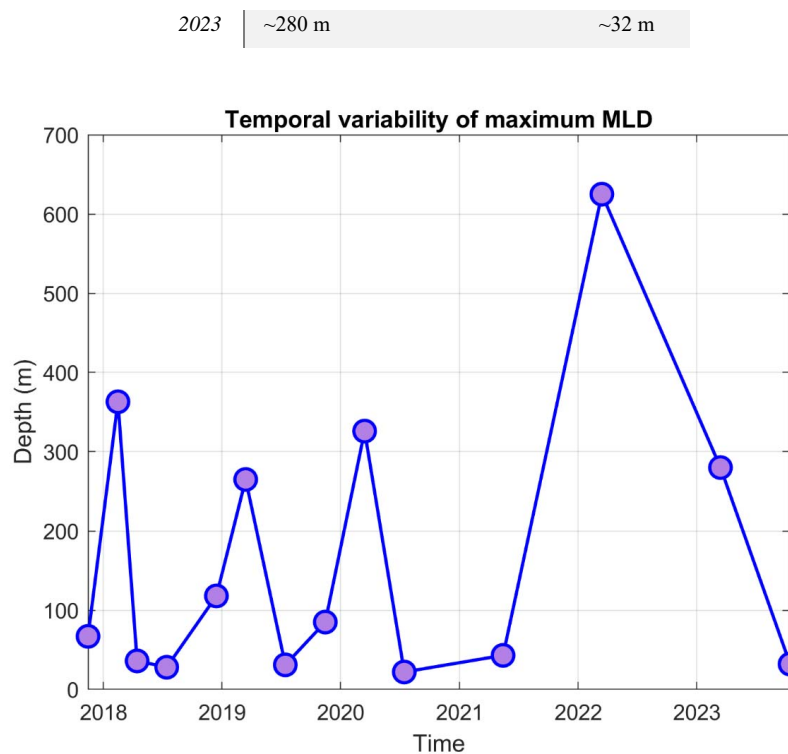
Using Copernicus Marine Med-MFC products, Teruzzi et al. (2024) detected that the mixed layer depth (MLD; calculated as the depth at which the density increases by  $0.01 \text{ kg m}^{-3}$  compared to the density at 10 m) exceeded 500 m on several occasions  
225 during late January and early March 2022 in the area southeast of Crete also developing or exceeding once the maximum value of 700 m, indicating intense dense convection and water-mass formation among the strongest events in recent decades. The impact of the 2022 cold spells on the north-central Aegean Sea was also demonstrated by Potiris et al. (2024), who showed that buoyancy losses during winter 2021–2022 were comparable to other major DWF years (1993–1994, 2002–2003, 2012) and suggest that the mixed layer deepened to 700–800 m around 20 March, according to model simulations. This intense cold  
230 atmospheric anomaly triggered as well the production of dense waters inside the Cretan Basin and altered the density stratification. As discussed in the following section, this exceptional event launched an abrupt reorganization of the Cretan deep-water layers, displacing TMW low salinity core below 1000 m.

Table 1: Maximum MLDs calculated for each glider mission

	Winter	Spring	Summer	Autumn
2017				~67 m
2018	~363 m	~36 m	~28 m	~118 m
2019	~265 m		~31 m	~85 m
2020	~326 m		~22 m	
2021			~43 m	
2022		~625 m		



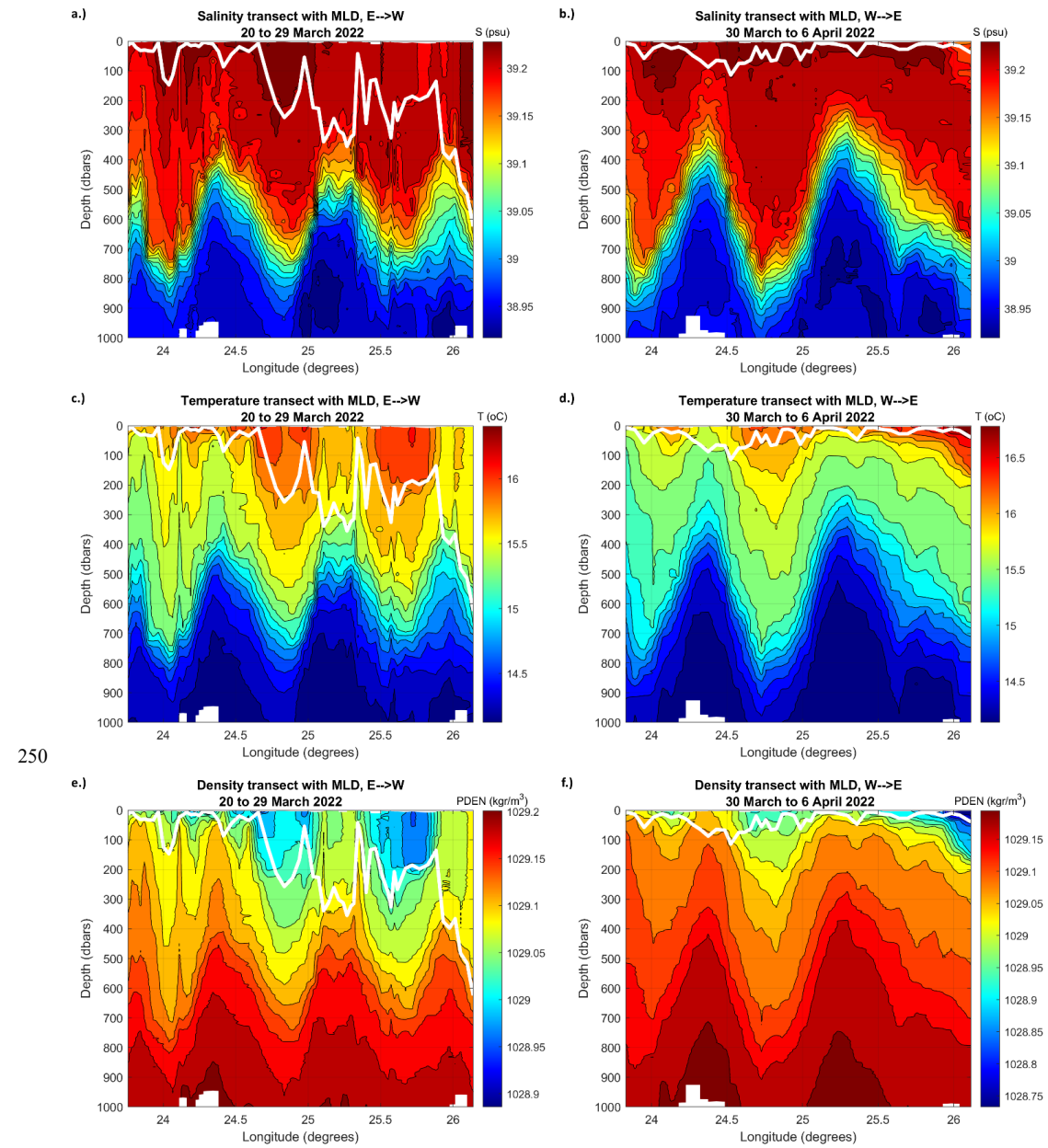
235



**Figure 7: Temporal variability of the mixed layer depth (MLD) maximum values in the Cretan Sea during 2017–2023, derived from glider observations. The seasonal cycle shows shallow MLDs in summer (<30 m), intermediate values during autumn (~100 m), and deepening during winter (~300 m), with the exception of winter 2022, when the MLD exceeded 600 m.**

240 In more detail, the glider captured a detailed snapshot of the intense convection event that occurred during winter 2022. Dense water formation was primarily observed in the eastern part along the east-to-west transect, suggested by the MLD that is deepening over 600 m eastwards in fig. 8a, c, e. The following glider transect, conducted in the opposite direction (west-to-east), revealed substantial changes in density stratification extending to the deeper layers (Fig.8b, d, f), along with the inflow of warmer and fresher surface waters spreading on the opposite direction from east to west. Fig. 9a presents the transect of density difference ( $\Delta\sigma_0$ ) between these two consecutive periods — 20–29 March 2022 (E→W transect) and 30 March–6 April 2022 (W→E transect)—capturing the evolution of the vertical density structure during the peak of the convection phase in the Cretan Sea. A rapid increase in density is evident in the eastern part of the glider transect, reaching approximately  $0.01 \text{ kg/m}^3$  over 900 m depth,  $\sim 0.03 \text{ kg/m}^3$  in  $\sim 700 \text{ m}$ ,  $\sim 0.07 \text{ kg/m}^3$  around 400 m and up to  $\sim 0.1 \text{ kg/m}^3$  in  $\sim 200 \text{ m}$  depth.

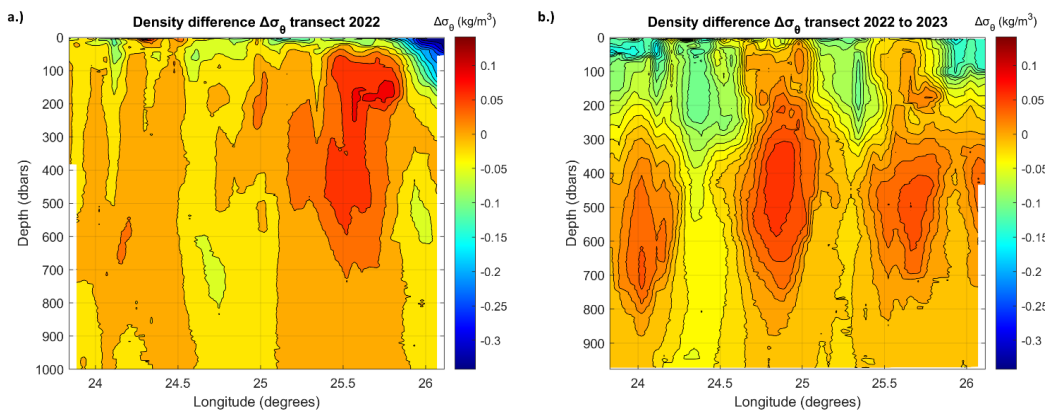
245





255 **Figure 8:** a) Salinity distribution along the east-to-west transect during winter 2022 (20–29 March 2022), and b) salinity along the  
 subsequent west-to-east transect (30 March–6 April 2022). The white line denotes the MLD, highlighting intensified dense-water  
 formation toward the east in panel (a), while panel (b) illustrates salinity changes down to ~600 m in the eastern part of the transect.  
 c and e.) East-to-west transects of temperature and density, respectively; and d and f.) the same variables for the west-to-east  
 transects. The formation of dense water triggers an increase in buoyant inflow at the surface in the eastern part of the transect.

260 The density difference field  $\Delta\sigma_0$ , shown in Fig. 9b for the period between March 2022 and March 2023, further highlights the  
 significant interannual variability observed in the water column in the intermediate and deeper layers. The reported density  
 alteration is associated with the occurrence of the strong convective event in winter 2022, which is suggested that initiated a  
 phase that provoked the recorded changes in winter 2023. The observed increase in density extends across the eastern, central  
 and western parts of the transect, indicating that convective events influenced the entire Cretan Sea. Density deviations reached  
 values of approximately 0.01–0.03 kg/m<sup>3</sup> at a depth of around 800 m and up to 0.06 kg/m<sup>3</sup> at a depth of around 500 m, which  
 further supporting the widespread impact of the intense convection episode in winter 2022.



265 **Figure 9:** a.) Transect of  $\Delta\sigma_0$  between two consecutive periods, 20–29 March 2022 and 30 March–6 April 2022. Positive  $\Delta\sigma_0$  values  
 indicate denser water during the latter period (30 March–6 April 2022), while negative values indicate lighter waters. b.) Transect  
 of  $\Delta\sigma_0$  between 20–29 March 2022 and 19–28 March 2023, showing interannual changes in the vertical density structure of the  
 Cretan Sea during late winter.

#### 4 Interannual variability in the surface, intermediate and deep layers

270 In this section we are going to examine the interannual variability of temperature, salinity and density, considering five (5)  
 characteristic depth layers in the vertical section sampled by the glider in order to investigate the variations of the water masses'  
 properties at each layer depth defined as 0–2 m, 2–70 m, 70–200 m, 200–600 m, 600–1000 m. The mean values of these  
 variables are calculated for all the missions per depth layer considering one transect of the glider from the eastern to the western  
 end. Then, the temporal evolution of the means is presented in Fig. 10. The vertical distribution of water masses is characterized  
 275 as follows.

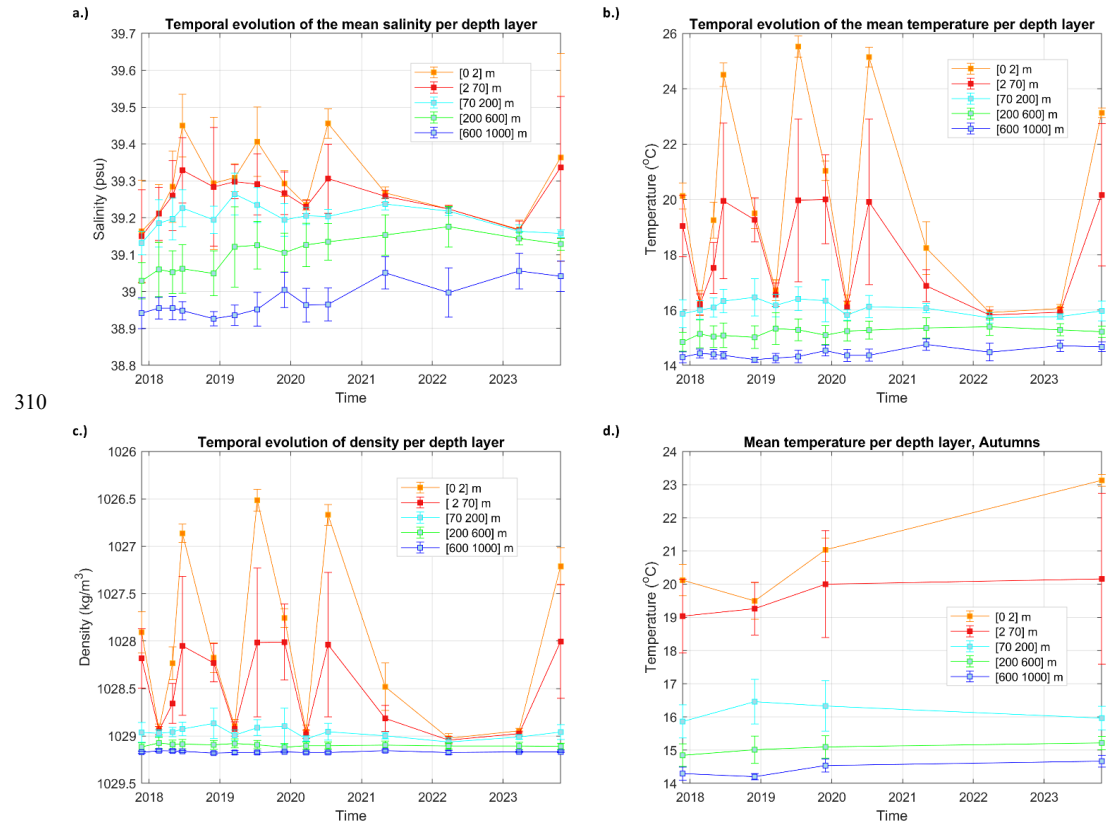


As previously noted, the surface and subsurface layers of the Cretan Sea are influenced mostly by LSW and in some cases by modified AW, which has become warmer and saltier on its way towards the Cretan Straights. Additional inflows from the northern Aegean also affect Cretan surface water properties, occasionally carrying the fresher BSW signature.

At intermediate depths, the Cretan basin hosts both CIW and LIW. LIW are formed mainly in the Rhodes Gyre region and 280 entering the Cretan Sea mainly through the Eastern Straights, (Theocharis et al., 1993; Velaoras et al., 2014). CIW are formed locally during winter convection and as we can see in Fig. 7b and Table 1 reach depths 260 to 360 m in a yearly basis. However, there are occasions of intense formation that reach deeper, such as in winter 2022 when mixing extended to 600 m. It is quite difficult to distinguish between these two water masses although the CIW as newly formed, has higher oxygen content, but densities that vary interannually however with hydrological characteristics similar to LIW. In the horizons under the LIW and 285 CIW lays the TMW which originates in the transient layers of the EMed between LIW and EMDW (Eastern Mediterranean Deep Water) and appears recurrently in the Cretan Sea as a compensation of dense water mass export from it (Theocharis et al., 1999b; Velaoras et al., 2015). TMW appears in the TS diagrams as the hump in the deeper layers over the 600 m (Fig. 5d). Below TMW, the deep layers are occupied by CDW (Fig. 5d), which were formed mostly during the EMT period and fill the deep basins of the Cretan Sea. Velaoras et al. (2021) has stated that no new deep water has been added to the deep Cretan 290 basins after the EMT event (1992–1995) as there has been no severe DWF episode since. During the glider missions, mixed layer depths reached up to ~600 m, a fact that indicates too that no deep convection events have occurred that would lead to the formation of new CDW. However, this requires further investigation, particularly in relation to the abrupt downward shift of TMW after 2022, which is examined in detail in the next section.

In Fig. 10, the temporal evolution of the temperature, salinity and density means and their respective standard deviation are 295 depicted, considering all the missions conducted during the 2017 – 2023 period (Fig. 10 a, b, c). Overall, it is deduced that seasonality has the greatest impact on the surface layers, as it is well presented during the first years of the glider missions, when we have undertaken a minimum of two/three missions per annum.

Fig. 10d shows the yearly temporal evolution of the mean temperature considering autumns exclusively, to illustrate the prolonged high temperatures following the summer of 2023. The Eastern Mediterranean experienced a hitherto exceptionally 300 hot and extended summer in 2023, with record-breaking heatwaves and prolonged periods of extreme temperatures (Copernicus Marine Service, 2023). The impact on sea surface temperature during autumn 2023, a year reported by Copernicus Climate Change Service (C3S) (2024) as the hottest on record until then, is evident in Fig. 10d. The mean surface temperature in autumn 2023 was ~2°C higher than the mean recorded in autumn 2020. Summer and early autumn 2023 were characterized by exceptionally high sea surface temperatures across the Mediterranean Basin. These temperatures were associated with one 305 of the most intense and prolonged marine heatwave events recorded in the region in the last four decades (Martellucci et al., 2025). The persistence of these anomalously warm conditions resulted in delayed destratification and record-high subsurface temperatures, as reflected in glider profiles from this period. In the Eastern Mediterranean, these increasingly persistent heat anomalies have the potential to disrupt established thermohaline patterns and alter key water-mass formation processes, placing additional stress on an already sensitive regional system.



315

**Figure 10: Temporal evolution of the mean values of salinity, temperature and density per depth layer (0 – 2 m, 2 – 70 m, 70 – 200 m, 200 – 600 m, 600 – 1000 m), considering the profiles on the glider transect. Means and the respective standard deviations shown in the panels a, b and d are calculated for each glider mission. The figure d is representing the temperature evolution considering autumns exclusively, in order to illustrate the extended high temperatures following the 2023 summer.**

The temporal evolution of the mean thermohaline properties shown in Fig. 10 demonstrates the seasonal signals in both temperature and salinity progressively weakening with depth. The upper ~70 m are strongly influenced by atmospheric forcing and display distinct seasonal variability. Below this layer the impact become moderate up to 200 m, still showing weakened signals linked to surface processes. Waters deeper than 200 m exhibit comparatively stable conditions with limited seasonal modulation.

320



#### 4.1 Long six years' trend in intermediate and deep layers

In order to have a closer look on the temporal evolution of the deeper layers, the vertical range was localized to the intermediate (200–600 m), and deep (600–1000 m) layers. For each layer, temporal means were computed and a linear regression was applied to evaluate long-term tendencies over the 6-year glider observational period as depicted in Fig. 11. While acknowledging the relatively short duration of the dataset and the incomplete year-round sampling — factors that prevent a robust climatic trend assessment — this approach provides valuable first-order indications of the direction and approximate magnitude of thermohaline evolution in the Cretan Sea.

Fig. 11 demonstrates the warming and salinification of the intermediate and deep layers of the Cretan Sea during the period 2017–2023. The mean temperature of the intermediate layer increased by  $0.0519 \pm 0.004$  °C per year, while the mean temperature of the deep layer increased by  $0.0678 \pm 0.004$  °C per year. The corresponding mean salinity fields are increasing by  $0.019 \pm 0.001$  and  $0.02 \pm 0.0009$  psu per year at intermediate and deep layers, respectively. During this period, the mean salinity of the intermediate and deep layers increased by ~0.1, while the corresponding mean temperature increased by ~0.37 °C and ~0.38 °C.

Additional trends are calculated in the 250, 400, 600, 1000 m depth levels of the E1M3A buoy (Fig. 2), for the exact time period of the glider operation, that is November 2017 to November 2023 (Fig. 12). The temperature and salinity trends for the above depths of the E1M3A buoy are presented in Table 2. The increasing values we observe with depth also in the glider data are consistent with these values.

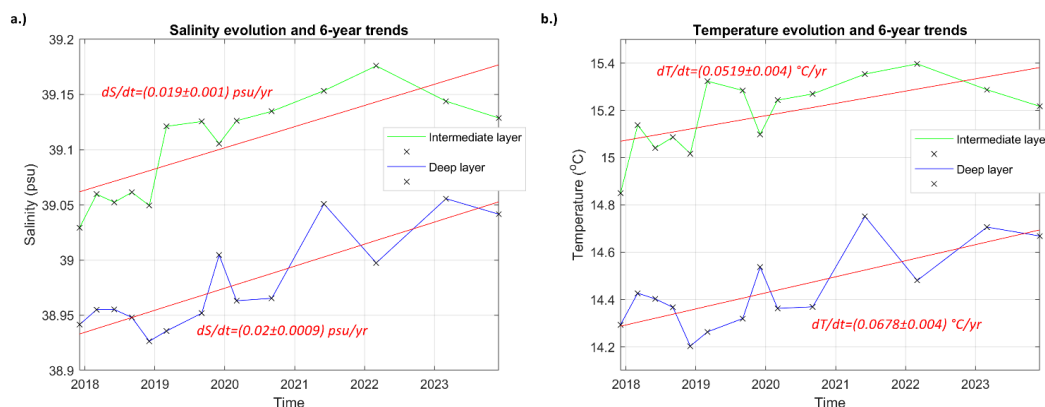
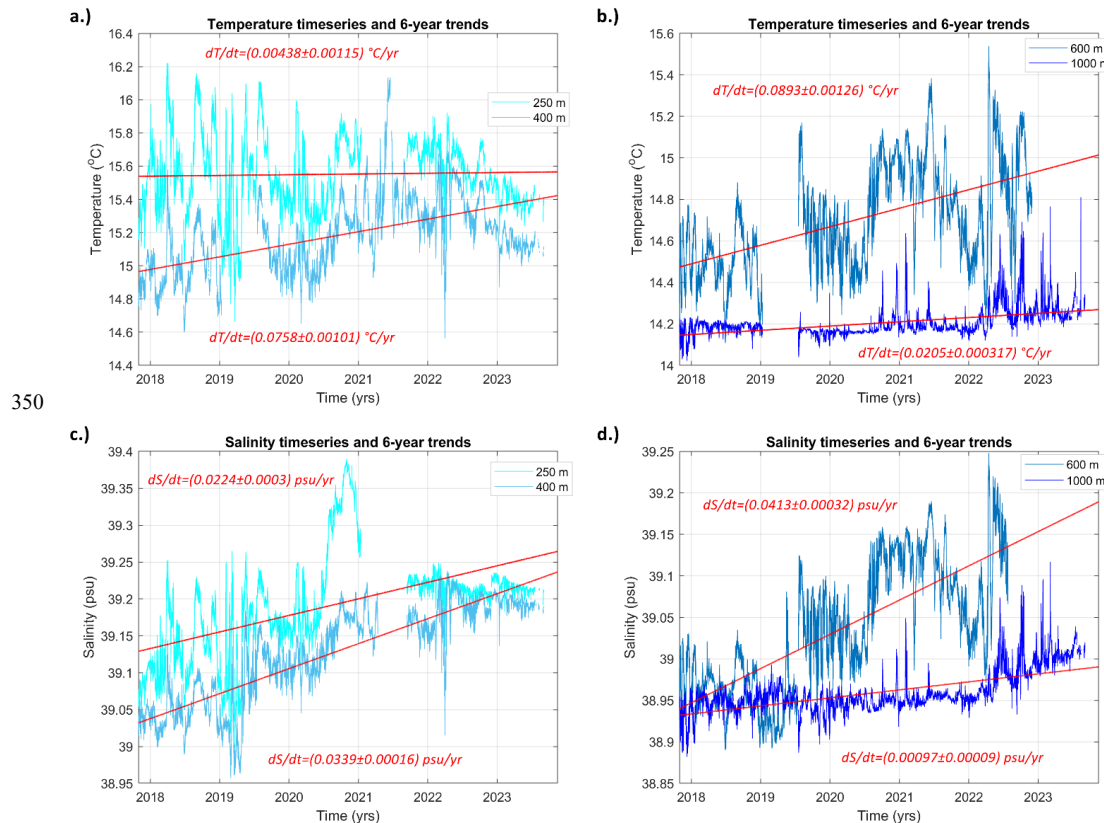


Figure 11: Temporal evolution of the mean temperature and salinity per depth layer (200–600 m, 600–1000 m) on the glider transect and the respective 6-year trend.

The recorded trends in the Cretan Sea seems to be a direct result of wider Mediterranean and global scale climatic trends, as well as short-term hydrological and circulation-related processes in the Eastern Mediterranean, as the periodic reversals



345 between cyclonic and anticyclonic modes of the Northern Ionian Gyre (NIG). Schroeder et al. (2017) demonstrated that the Mediterranean Sea is a particularly sensitive marginal sea to changes in external forcing and extremely responsive to climate change compared to the global ocean. They reported mean trends in LIW/CIW temperature and salinity in the Sicily Channel (400 m) over a 22-year period: 0.024 °C per year and 0.006 psu per year, respectively (see Table 2). At the same time, the C3S (2025) reports a global scale temperature trend of 0.009 °C per year for the upper 700 m over 31 years.



**Figure 12: Temporal evolution of temperature and salinity on the E1M3A intermediate and deep levels (250, 400, 600 and 1000 m) and the respective 6 – year trend.**

355 Previous studies have reported trends in the western, central and eastern Mediterranean Sea (Table 2), derived from in situ data. Regarding the Eastern Mediterranean Sea, Ozer et al. (2022) report long-term warming and salinification trends with yearly rates of 0.048 °C and 0.006, respectively. These were derived from a comprehensive analysis of decadal thermohaline



variability (March 2011 to June 2021) in the surface and intermediate layers of the East Levantine basin coastal waters. Skliris et al. (2018), on the other hand, report decadal salinity trends of  $0.0109 \pm 0.006$  and  $0.0071 \pm 0.002$  for depths of 150–600 m and 600 – 1000 m, respectively. They conclude that salinification of the Mediterranean basin is driven by changes in the regional water cycle rather than changes in salt transport through the straits.

Furthermore, Kubin et al. (2023) calculated a temperature trend of  $0.041 \pm 0.012 \text{ }^{\circ}\text{C}\cdot\text{yr}^{-1}$  for the upper 700 m of the Mediterranean Sea using Argo floats. The Western Mediterranean Sea (5–700 m) is warming faster, with an increase in temperature at a rate of  $0.070 \pm 0.015 \text{ }^{\circ}\text{C}\cdot\text{yr}^{-1}$ .

The trends deduced in this study for the Cretan Sea appear consistent with those in the western and central Mediterranean. Barceló-Llull et al. (2019) reported a long-term trend in the core of the LIW temperature (300–700 m) in the Mallorca Channel, calculated from glider data, of  $0.044 \pm 0.002 \text{ }^{\circ}\text{C}\cdot\text{yr}^{-1}$ , and an increment in the core temperature of the Western Mediterranean Water (WIW) (100–300 m) of  $0.064 \pm 0.002 \text{ }^{\circ}\text{C}\cdot\text{yr}^{-1}$ . Schroeder et al. (2017) reported a similar temperature trend of  $0.064 \text{ }^{\circ}\text{C}\cdot\text{yr}^{-1}$  at 400 m in the Sicily Channel, analysing temperature and salinity time series from 2010 to 2016. In the Ligurian Sea, Margrier et al. (2020) observed a similar warming trend of  $+0.06 \pm 0.01 \text{ }^{\circ}\text{C}\cdot\text{yr}^{-1}$  and salinification of  $+0.012 \pm 0.02 \text{ yr}^{-1}$  in the LIW from 2007 to 2017. Similar increase rates in temperature were observed in the Cretan Sea to those in the Central and Western Mediterranean Sea, while faster increases in salinity were evident. This may support the salt and heat transport from east to west in the Mediterranean, as described by Schroeder et al. (2017) and corroborated by Barceló-Llull et al. (2019). All of the aforementioned research demonstrates a steady increasing trend in temperature and salinity at these depths within the Mediterranean basin, with no clear indication of significant variations between its different regions. Nevertheless, the rapid response to climate change in the marginal Mediterranean Sea is once again demonstrated (Schroeder et al., 2017), as the reported warming in the Cretan Sea is over the one order of magnitude greater than that reported for the global ocean in the upper 700 m:  $0.29 \pm 0.004 \text{ }^{\circ}\text{C}$  from 1993 to 2024 (C3S, 2025).

Table 2: Temperature and salinity long term yearly trends and associated errors reported for various spots in the Mediterranean Sea for intermediate and deep layers.

	Period	Reference	Region	Temperature $\text{ }^{\circ}\text{C}\cdot\text{yr}^{-1}$	Salinity $\text{psu}\cdot\text{yr}^{-1}$
<b>Barceló-</b> <b>Llull B. et al.</b> <b>(2019)</b>	2011- 2018	WIW (100-300m) LIW (300-700m)	Mallorca channel	$0.064 \pm 0.002$ $0.044 \pm 0.002$	$0.016$
<b>Schroeder</b> <b>K. et al.</b> <b>(2017)</b>	2010- 2016	400 m channel	Sicily	$0.064$	$0.014$



<b>Schroeder</b>	1993-	400 m	Sicily	0.024	0.006
<b>K. et al.</b>	2016		channel		
<b>(2017)</b>					
<b>Margirier F.</b>	2007-	LIW	Ligurian	0.06±0.01	0.012±0.02
<b>et al. (2020)</b>	2017		Sea		
<b>Kubin E. et al. (2023)</b>	2005-2020	5-700 m	MED	0.041±0.012	
			WMED	0.070±0.015	
<b>Ozer T. et al. (2022)</b>	2011-2021	Coastal waters Shallow/interm. 0-150	East	0.048	0.006
<b>Skliris et al. (2018)</b>	1950-2015	150-600 m >600 m	EMED (1950-2015)		0.00109 ± 0.0006 0.00071 ± 0.0002
<b>This study (glider transect means)</b>	2017-2023	200-600 m >600 m	Cretan Sea	0.0519±0.004 0.0678±0.004	0.019±0.0010 0.020±0.0009
<b>This study (timeseries)</b>	2017-2023	250 m 400 m 600 m 1000 m	Cretan Sea	0.00438±0.00115 0.0758±0.00101 0.0893±0.00126 0.0205±0.000317	0.0224±0.0003 0.0339±0.00016 0.0413±0.00032 0.00097±0.00009

#### 4.2 Identifying deviations from the recent climatology

The above means and long-term trends from 2017 to 2023 were estimated to reveal the variability of the hydrological characteristics of the Cretan Sea recorded during the glider missions in that specific time period. Furthermore, in order to highlight changes in relation to the Cretan Sea's past state, mean salinity and temperature deviations were calculated in relation to the most recent climatology (Iona A. et al., 2018). The seasonal climatology for winters in the most recent period (2000–2015) was selected to be correlated with the means calculated from winter glider missions conducted during the period 2018–2023. In order to highlight the increase in ocean variables recorded during the glider analysis period compared to the climatology period of 2000–2015, salinity, temperature and density anomalies were derived at each depth of the climatology grid, from the water surface to 1000 m (5, 10, 30, 75, 200, 400, 700 and 1000 m). The temperature deviation is estimated to be around 0.4–0.6 °C in the first 400 m, decreasing to almost zero at 1000 m (Fig. 13a). This indicates a significant overall



increase in water temperature in the first 400 m of the Cretan Sea, where it remains relatively stable. However, this increase becomes less significant at greater depths, reaching small values at 1000 m.

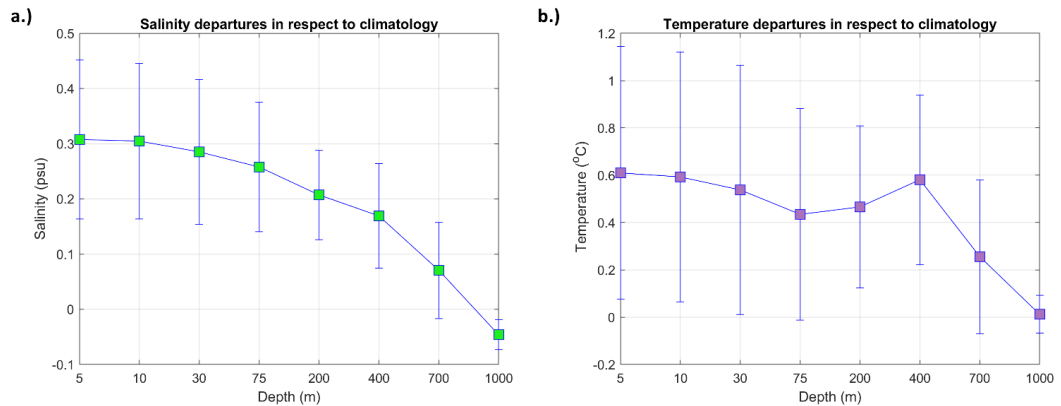


**Figure 13: Deviation of the mean fields of salinity (a) and temperature (b) calculated for all winter glider missions (2018 to 2023) at each depth in relation to the respective climatology for the period from winter 2000 to winter 2015.**

As shown in Fig. 13b, the salinity deviation decreases gradually from 0.31 at the surface to  $-0.05$  at 1000 m. The considerable 400 salinity and temperature increases observed in the upper 400 m are consistent with winter convection, which annually forms CIW and regulates the downward heat and salt transport from the surface to intermediate depths.

#### 4.3 Temporal Evolution of TMW Transformation

Velaoras et al. (2015) demonstrated that the occurrence of TMW in the Cretan Basin follows a recurrent pattern strongly associated with dense water formation events in the southern Aegean Sea. When new dense water formation causes an outflow 405 of dense water through the Cretan Straits into the Eastern Mediterranean, a corresponding TMW inflow occurs in the Cretan Sea to compensate for the outflow. The authors also state that TMW intrusions in the Cretan Sea are valuable for tracing and evaluating dense water formation events in the area.

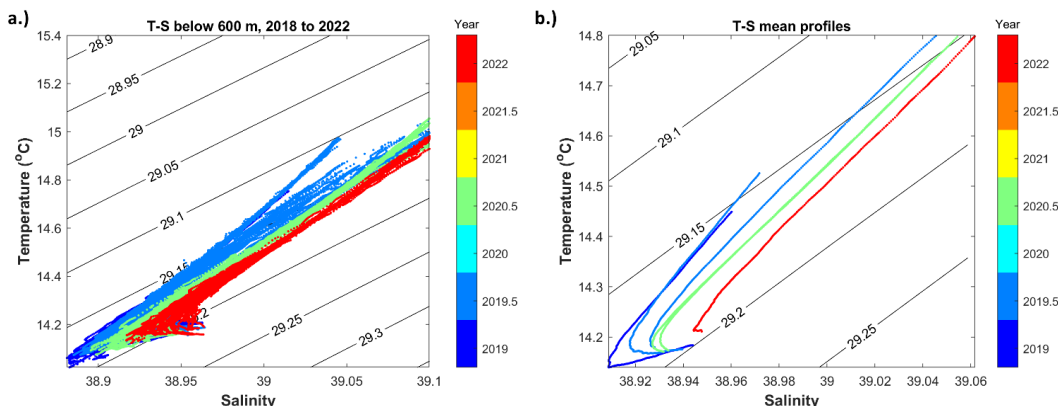
According to Theocharis et al. (1999a), the TMW's presence in the Cretan Sea has been attributed to the EMT event, appearing as a distinct intermediate layer of water with minimum temperature and salinity and alongside the newly formed CDW, it 410 became a significant structural component of the South Aegean Sea. Following the EMT's post -period, TMW masses' core depth within the Cretan Sea gradually increased from 600 to over 1200 dbar over the subsequent decade up to 2012. At the same time, TMW core salinity increased by 0.1, as detailed in Velaoras et al. (2015). Velaoras (2014) and Vervatis et al. (2009) attribute the recession of the TMW salinity 'hump' towards greater depths and salinities to water mass exchanges occurring 415 between the Cretan Sea and the Mediterranean Sea, as well as to mixing processes in the layers of Cretan water masses. Double diffusion (salt fingering) processes between the warm and salty overlying LIW layer and the colder and less salty TMW,



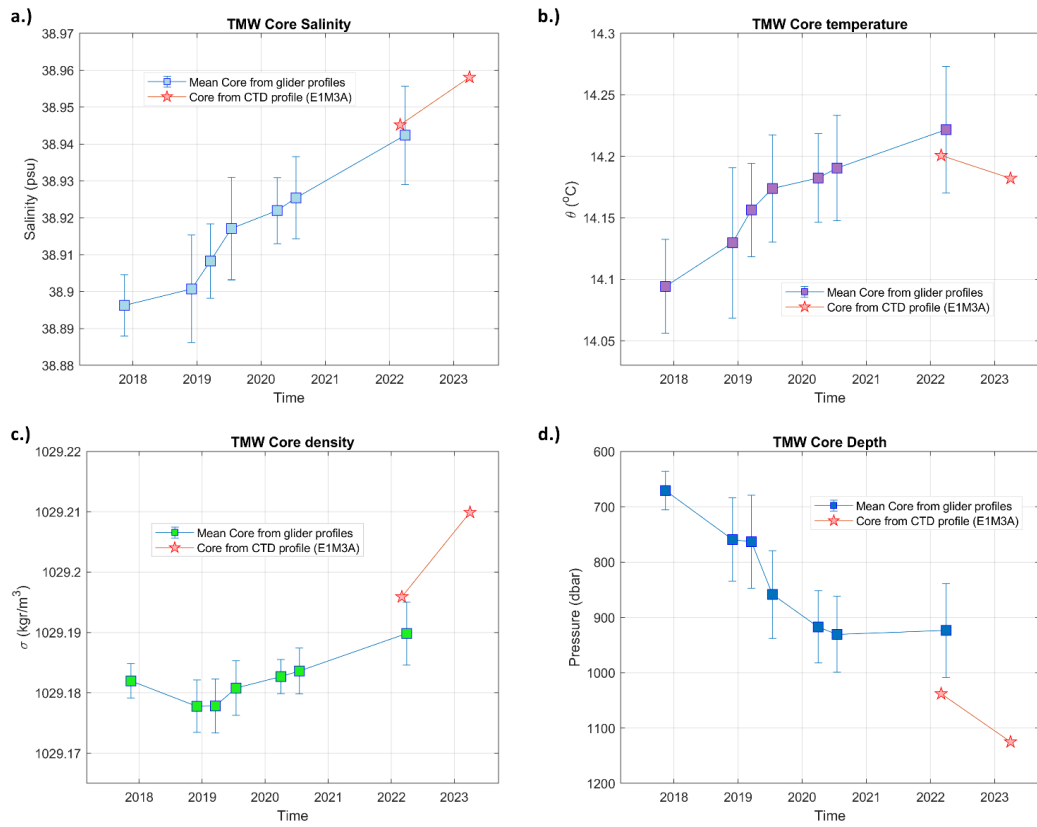
contribute to the TMW erosion during stagnation periods (Velaoras et al., 2025). A new TMW intrusion is reported to have started in 2012, culminating in 2014. This recent TMW accumulation is found in the Cretan layers between 500 and 1000 dbar, with the core at 740 dbar and salinity ranging from 38.96 to 38.98 (Velaoras et al., 2015). Kassis et al. (2016) also described a new TMW intrusion at 200–300 m depth during November/December 2013.

420 This post-EMT TMW signal was detected during the initial glider mission at the end of 2017, appearing below 600 m in the eastern part of the transect. TMW was last observed by the glider within the 1000 m layer in March 2022, while by March 2023 it had descended to a depth of ~1150 m, as depicted in the CTD casts conducted down to the bottom.

During the glider observations period, the TMW has gradually moved down into deeper layers, altering its low-salinity core and becoming more saline and warm. The change in TMW properties is initially observed in the T – S diagrams centered 425 between 600 and 1000 m, considering the full dataset of glider missions, as depicted in Fig. 14. The evolution of the TMW over the years has followed the same pattern extensively described by Velaoras et al. (2015) during the stagnation period: the TMW layer has progressively deepened and eroded, increasing its core salinity and depth. To evaluate the deepening of the TMW, as well as its salinification and warming evident from 2017 to 2022, we calculated the mean core depth, salinity, temperature, and density for each mission, as well as the corresponding standard deviation in each case (Fig. 15). Profiles 430 reaching 1000 m were used and the TMW was traced as a salinity minimum between 500 and 1000 m. Late missions in which the TMW was absent were excluded from the calculations, while the eastern part of the first mission in 2017, in which the TMW was evident between 600 m and 700 m, was included.



435 **Figure 14: a.) T – S diagram showing the TMW transformation during the period November 2018 – March 2022 in the horizon of 600 m to 1000 m depth. b.) Mean profiles for each glider mission are considered.**



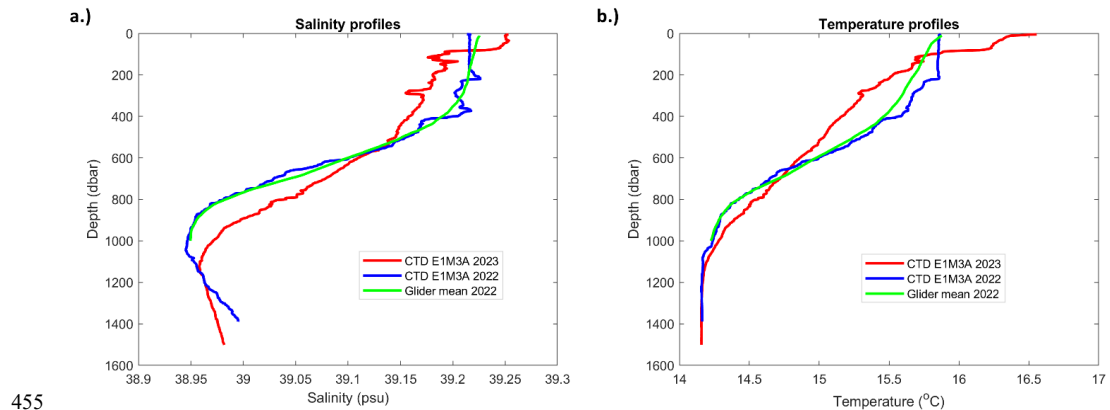
**Figure 15: Temporal evolution of TMW core salinity (a), temperature (b), density (c), and depth (d). Core values are shown as the mean for each glider mission, with error bars representing the standard deviation. Red stars indicate the core values measured during the winters of 2022 and 2023 from CTD casts at the E1M3A position (Fig. 2).**

Fig. 15 reveals a progressive deepening of the TMW core by approximately 250 m over the period 2017 – 2022 (derived by glider data), accompanied by a salinity reduction of  $\sim 0.046$  psu and a temperature increase of  $\sim 0.125$   $^{\circ}$ C. Considering the CTD casts at the E1M3A position, the core TMW properties during the study period (2017–2023) show the following changes: a deepening of approximately 450 m, an increase of about 0.062 psu in salinity, and  $\sim 0.088$   $^{\circ}$ C in temperature. Fig. 16 further illustrates the evolution during the last year of the study period (03/2022 – 03/2023) by appending the E1M3A CTD profiles from March 2022 and March 2023—extending down to the bottom—to the mean glider profile of winter 2022. The downward displacement of the characteristic TMW ‘hump’ becomes more evident in this representation, due to the inclusion of depths below 1000 m that are not reached by the glider. These observations indicate that notable modifications in the properties of

445



450 the deep water masses occurred during the final year of the study period, following the strong convective event of winter 2022. This finding underscores the need for further investigation into the extent of dense-water formation that appears to have taken place in parts of the Eastern Mediterranean – southeast of Crete (Terruzzi et al., 2024), north - central Aegean Sea (Potiris et al., 2024) – as well as its impact on the redistribution and transformation of deep waters within the Cretan basin. As shown in Fig. 16, these changes appear to propagate all the way to the bottom at the central Cretan Sea site (E1M3A position).



455 **Figure 16: Salinity (a) and Temperature (b) profiles from CTD casts in the position of E1M3A (Fig.2) for two consecutive years: 03/03/2022 (blue line) plotted with the glider mean profile of the March 2022 mission and 01/04/2023 (red line). The deepening of the salinity ‘hump’ below 1000 m between winter 2022 and winter 2023 is evident in panel a.**

460 Fig. 17 shows profiles obtained at two different locations in the Cretan Sea (E1M3A and East depression in Fig.2) during almost the same period (March–April 2023). TMW properties differ among the sampled areas, suggesting variability in water-mass “maturity,” i.e., the degree of transformation through mixing processes. In the eastern and deeper part of the basin, TMW appears to be less modified, characterized by lower salinity values. This water mass may represent an older TMW, potentially 465 accumulated and preserved in the deep, more isolated eastern sub-basin of the Cretan Sea following the post-EMT reorganization, hypothesis that is interesting to further examine. The eastern depressions reach depths of up to ~2000 m, facilitating the retention of these older layers from external dynamical influences.

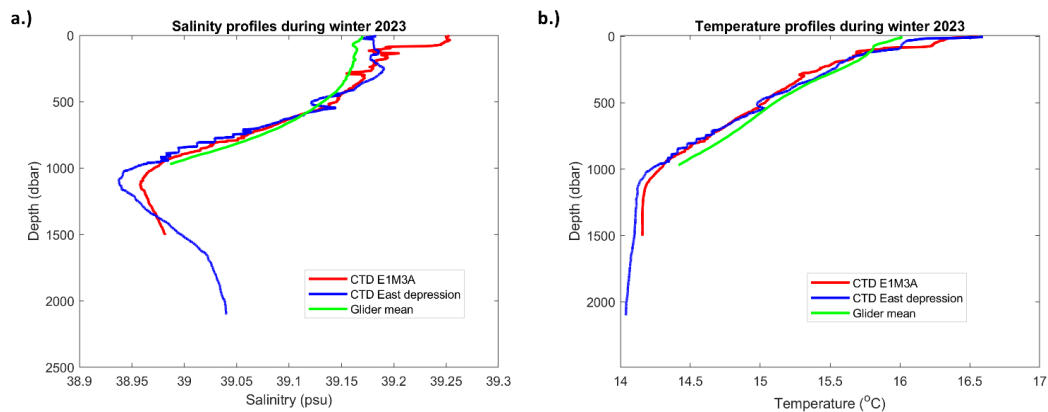


**Figure 17: Track the TMW in March 2023 using CTDs in the Cretan region, plotted alongside the mean glider mission profile calculated from east to west end across the transect. Position of the CTD casts and the glider transect are presented in Fig. 2. The**

470 **salinity minimum is depicted as higher in the E1M3A profile than in the eastern Cretan depression.**

## 5 Conclusions and discussion

This study presents an analysis of six years (2017 – 2023) of sustained glider observations collected as part of the endurance line established in the Cretan Sea, a component of the Poseidon Monitoring and Forecasting System (<https://poseidon.hcmr.gr>).

The data collected during this period were analysed to study the temporal and spatial variability of physical parameters and 475 the mesoscale phenomena to be present in the area. The Cretan Sea is a key component of the Eastern Mediterranean thermohaline circulation, and is one of the three principal dense water formation areas, along with the Levantine and Adriatic Seas. The EMT highlighted the importance of the Cretan Sea, demonstrating its role as a major heat and salt storage area that accumulates, transforms and redistributes water masses originating from the Aegean sub-basins, the Levantine Sea and the Ionian Sea, acting as an active intermediate and occasionally deep water mass source (Theocharis et al., 1993; Velaoras et al., 480 2014).

Analysis of the salinity and temperature dataset collected between 2017 and 2023 reveals that intermediate waters formed annually, ventilating water layers down to 260 – 360 m during winters, except in winter 2022, when the Cretan Sea experienced a strong mixing event triggered by intense cold spells. The mixed layer, as captured by the glider extended below 600 m inside the Cretan basin, providing newly formed waters that reached almost to the deep layers. Furthermore, glider observations 485 indicate a rapid density increase during winter 2022 and long-lasting changes that persisted into 2023. Dense mixing events were also reported by Teruzzi et al. (2024) during early spring 2022 in the area southeast of Crete, who described an anomalous deep – mixing and bloom event in the south eastern Mediterranean Sea as well as by Potiris et al. (2024), who reported that the mixed layer deepened to 700–800 m around mid-March in the North Aegean Sea, indicating that winter 2022 was



anomalous for the eastern Mediterranean. TMW core residing in the Cretan Sea was found in winter 2023 to be 200 m deeper  
490 than winter 2022 and 0.016 psu saltier, while over the entire study period (six years) the gradual deepening of TMW was approximately 450 m and its salinification 0.062 psu. The conclusion is that winter 2022 convection was sufficient to marginally produce deep waters, but not to sustain full deep-water formation. Nevertheless, even in the following year vertical mixing did not reach the deepest layers to ventilate with newly formed CDW. Instead, it contributed to accelerating the downward shift of the TMW occupying the area, driving it below 1000 m, as documented by CTD observations in the area.  
495 As the Cretan Sea functions as a dynamic intermediary in the thermohaline circulation of the Eastern Mediterranean, interacting with neighbouring basins through the east and west Cretan Straits, these results suggest that the extent of water formation during the anomalous winter of 2022 and its effects on the entire eastern Mediterranean require further investigation. The 2023 marine heatwave, reported by C3S (2024) as the hottest year on record to that point, was captured in the glider data, with mean surface temperature during autumn 2023 approximately 2 °C higher than the previously recorded mean for autumn  
500 2020. Additionally, the entire glider dataset showed progressive warming and increased salinity in the intermediate and deep layers during the study period, demonstrating a steady upward trend with mean temperature increases of about 0.05–0.07 °C per year and salinity increases of about 0.02 per year. These trends are consistent with broader Mediterranean observations but exceed global ocean averages of  $0.29 \pm 0.004^\circ\text{C}$  from 1993 to 2024 in the upper 700 m (C3S, 2025), confirming the strong regional response to climate change (Schroeder et al., 2017). Comparisons with climatological data (2000–2015) revealed  
505 temperature deviations of +0.4 to +0.6 °C in the upper 400 m and salinity deviations of approximately +0.3 at the surface, gradually decreasing with depth to -0.05 at 1000 m. The increase in temperature and salinity in the first 400 m is associated with winter convection that produces intermediate waters annually and transports heat and salt from the surface to the intermediate layers. Furthermore, the marginal salinity increase at 700 m (0.07 psu) and decrease at 1000 m (-0.05 psu) could be attributed to the effect of the low salinity TMW and its downward displacement from intermediate to deep layers, especially  
510 after the anomalous winter of 2022. It should be noted, that the substantial increase in salinity of the surface-layers in the Cretan Sea between 2017 and 2023 raises questions about its effect on local water mass formation processes during intense winter cooling and the atmospheric conditions necessary to trigger EMT-like events. It also raises questions about the long – term interdependencies between warming and salinification as regulators of Eastern Mediterranean circulation.

#### Data availability

515 Glider and CTD datasets, as well as satellite data used in this study are available here:  
<https://doi.org/10.5281/zenodo.1807623>.  
E1M3A (61277) fixed buoy time series data and glider data are available through the Copernicus Marine Service IN-SITU TAC (<https://marineinsitu.eu/dashboard/>).  
Mediterranean Sea-Temperature and Salinity Seasonal Climatology for the period 2000–2015, can be found here:  
520 <https://doi.org/10.5281/zenodo.1146966>.



#### Author contributions

Conceptualization: EB and LP; data curation: SV, DB, EB, GA and MP; formal analysis: EB, DB, GA and NS; funding acquisition: LP and GP; investigation: all authors; methodology, EB, DB, GA, NS, SV; resources: LP; software: SV, GA, DB and EB; supervision: LP; validation: LP and GP; visualization: EB and DB; writing – original draft preparation: EB; writing – review and editing: EB, DB, LP and GP.

#### Competing interests

The authors declare that they have no conflict of interest.

#### Disclaimer

Copernicus Publications remains neutral with regard to jurisdictional claims made in the text, published maps, institutional affiliations, or any other geographical representation in this paper. While Copernicus Publications makes every effort to include appropriate place names, the final responsibility lies with the authors. Views expressed in the text are those of the authors and do not necessarily reflect the views of the publisher.

#### Acknowledgements

We would like to acknowledge the valuable contribution of our co-author, S. Velanas, to the establishment of the Poseidon glider facility, together with E. Bourma and D. Ballas. We would also like to thank M. Pettas and S. Michelinakis for their support during glider deployments and recoveries, and for providing laboratory facilities for glider preparation and testing. Finally, we would like to thank Dr. Dimitris Velaoras for his valuable advice and fruitful discussions.

#### Financial support

This research was supported by the HIMIOFoTS project (MIS 5002739) from 2017 to 2021. HIMIOFoTS was implemented under the Action “Reinforcement of the Research and Innovation Infra-structure”, funded by the Operational Programme “Competitiveness, Entrepreneurship and Innovation” (NSRF 2014–2020) and co-financed by Greece and the EU. Glider operations and research conducted during 2022 and 2023 were supported by HCMR funds.



## References

Barceló-Llull, B., Pascual, A., Ruiz, S., Escudier, R., Torner, M., and Tintoré, J.: Temporal and spatial hydrodynamic variability in the Mallorca channel (western Mediterranean Sea) from 8 years of underwater glider data, *Journal of Geophysical Research: Oceans*, 124, 2769–2786, <https://doi.org/10.1029/2018JC014636>, 2019.

Bourma, E., Perivoliotis, L., Petihakis, G., Korres, G., Frangoulis, C., Ballas, D., Zervakis, V., Tragou, E., Katsafados, P., Spyrou, C., Dassenakis, M., Poulos, S., Megalofonou, P., Sofianos, S., Paramana, T., Katsaounis, G., Karditsa, A., Petrakis, S., Mavropoulou, A.-M., ... Zissis, N.: The Hellenic Marine Observing, Forecasting and Technology System—An Integrated Infrastructure for Marine Research. *Journal of Marine Science and Engineering*, 10(3), 329, <https://doi.org/10.3390/jmse10030329>, 2022.

Copernicus Climate Change Service (C3S), Climate Indicators, Ocean heat content indicator, <https://climate.copernicus.eu/climate-indicators/ocean-heat-content>, Last updated 15 April 2025.

Copernicus Climate Change Service: 2023 is the hottest year on record, with global temperatures close to the 1.5 °C limit, <https://climate.copernicus.eu/copernicus-2023-hottest-year-record> (last access: 23 December 2025), 2024.

Copernicus Marine Service: The 2023 Northern Hemisphere Summer Marks Record-Breaking Oceanic Events, <https://marine.copernicus.eu/news/2023-northern-hemisphere-summer-record-breaking-oceanic-events>, (last access: 23 December 2025), 2023.

Copernicus Marine Service: European Seas Gridded L4 Sea Surface Heights and Derived Variables – Reprocessed Product, <https://doi.org/10.48670/moi-00141>, 2024.

de Boyer Montégut, C., Madec, G., Fischer, A. S., Lazar, A., and Iudicone, D.: Mixed layer depth over the global ocean: An examination of profile data and a profile-based climatology, *J. Geophys. Res.-Oceans*, 109, C12003, <https://doi.org/10.1029/2004JC002378>, 2004.

EGO gliders data management team: EGO gliders NetCDF format reference manual, Ifremer, <https://doi.org/10.13155/34980>, 2025a.

Ego Gliders Data Management Team: EGO gliders Quality Control tests on timeseries and profiles data, Ifremer, <https://doi.org/10.13155/51485>, 2025b.

EMODnet Bathymetry Consortium: EMODnet digital bathymetry (DTM 2016), in EMODnet bathymetry consortium, <http://dx.doi.org/10.12770/c7b53704-999d-4721-b1a3-04ec60c87238>, 2016.

Gertman, I., Ovchinnikov, I., Popov, Y.: Deep convection in the eastern basin of the Mediterranean Sea, *Oceanology* 34 (1), 19–25, 1994.

IOC, SCOR, and IAPSO: The international thermodynamic equation of seawater – 2010: Calculation and use of thermodynamic properties of seawater, IOC Manuals and Guides No. 56, UNESCO, 2010.



Iona, A., Theodorou, A., Watelet, S., Troupin, C., Beckers, J.-M., and Simoncelli, S.: Mediterranean Sea Hydrographic Atlas: towards optimal data analysis by including time-dependent statistical parameters, *Earth Syst. Sci. Data*, 10, 1281–1300, <https://doi.org/10.5194/essd-10-1281-2018>, 2018.

Kassis, D., Krasakopoulou, E., Korres, G., Petihakis, G., Triantafyllou, G.: Hydrodynamic features of the South Aegean Sea as derived from Argo T/S and dissolved oxygen profiles in the area, *Ocean Dynamics*, 1-18, <http://dx.doi.org/10.1007/s10236-016-0987-2>, 2016.

Klein, B., Roether, W., Manca, B.B., Bregant, D., Beitzel, V., Kovacevic, V., Luchetta, A.: The large deep water transient in the Eastern Mediterranean, *Deep-Sea Res. Part I Oceanogr. Res. Pap.* 46 (3), 371e414. [https://doi.org/10.1016/S0967-0637\(98\)00075-2](https://doi.org/10.1016/S0967-0637(98)00075-2), 1999.

Kontoyiannis, H., Theocharis, A., Balopoulos, E., Kioroglou, S., Papadopoulos, V., Collins, M., Velegrakis, A.F., Iona, S., Water fluxes through the Cretan Arc Straits, Eastern Mediterranean Sea: March 1994 to June 1995, *Progr. Oceanogr.*, Vol. 44 (4), 511–529, [http://dx.doi.org/10.1016/S0079-6611\(99\)00044-0](http://dx.doi.org/10.1016/S0079-6611(99)00044-0), 1999.

Krokos, G., Velaoras, D., Korres, G., Perivoliotis, L., and Theocharis, A.: On the continuous functioning of an internal mechanism that drives the Eastern Mediterranean thermohaline circulation: The recent activation of the Aegean Sea as a dense water source area, *J. Mar. Syst.*, 129, 484–489, <https://doi.org/10.1016/j.jmarsys.2013.10.002>, 2014.

Kubin, E., Menna, M., Mauri, E., Notarstefano, G., Mieruch, S. and Poulain, P.M.: Heat content and temperature trends in the Mediterranean Sea as derived from Argo float data. *Front. Mar. Sci.* 10:1271638. <https://doi.org/10.3389/fmars.2023.1271638>, 2023.

Margirier, F., Testor, P., Heslop, E. et al.: Abrupt warming and salinification of intermediate waters interplays with decline of deep convection in the Northwestern Mediterranean Sea, *Sci Rep* 10, 20923, <https://doi.org/10.1038/s41598-020-77859-5>, 2020.

Martellucci, R., Tiralongo, F., Darmaraki, S.F, D'Alessandro, M., Mancinelli, G., Mancini, E., Simonini, R., Menna, M., Pirro, A., Borme, D., Auriemma, R., Graziano, M., and Mauri, E.: Mediterranean marine heatwave 2023: ecosystem and fisheries impacts in Italian waters, 9th edition of the Copernicus Ocean State Report (OSR9), Volume 6-osr9, <https://doi.org/10.5194/sp-6-osr9-9-2025>, 2025

Ozer, T., Gertman, I., Gildor, H.: Thermohaline temporal variability of the SE Mediterranean coastal waters (Israel) -long-term trends, seasonality, and connectivity, *Front. Mar. Sci.* 8, 799457, <https://doi.org/10.3389/fmars.2021.799457>, 2022.

Pinardi, N., Estournel, C., Cessi, P., Escudier, R., Lyubartsev, V.: Dense and deep water formation processes and Mediterranean overturning circulation, *Oceanography of the Mediterranean Sea*, Elsevier, 209-261, <https://doi.org/10.1016/B978-0-12-823692-5.00009-1>, 2023.

Potiris, M., Mamoutos, I. G., Tragou, E., Zervakis, V., Kassis, D., and Ballas, D.: Dense Water Formation in the North-Central Aegean Sea during Winter 2021–2022, *Journal of Marine Science and Engineering*, 12, 221, <https://doi.org/10.3390/jmse12020221>, 2024.



Roether, W., Manca, B.B., Klein, B., Bregant, D., Georgopoulos, D., Beitzel, V., Kovacevic, V., Luchetta, A.: Recent changes in Eastern Mediterranean deep waters, *Science*, 271, pp. 333-335, <https://doi.org/10.1126/science.271.5247.333>, 1996.

Roether, W., Klein, B., Manca, B.B., Theocharis, A., Kioroglou, S.: Transient Eastern Mediterranean deep waters in response to the massive dense-water output of the Aegean Sea in the 1990s, *Progress in Oceanography*, 74 (4), pp. 540-571, <https://doi.org/10.1016/j.pocean.2007.03.001>, 2007.

Schroeder, K., Chiggiato, J., Josey, S.A. et al.: Rapid response to climate change in a marginal sea. *Sci Rep* 7, 4065, <https://doi.org/10.1038/s41598-017-04455-5>, 2017.

Skliris, N., Zika, J.D., Herold, L. et al.: Mediterranean Sea water budget long-term trend inferred from salinity observations, *Clim Dyn* 51, 2857–2876, <https://doi.org/10.1007/s00382-017-4053-7>, 2018.

Sur, H. L., Özsoy, E., & Unluata, U.: Simultaneous deep and intermediate depth convection in the Northern Levantine Sea, winter 1992, *Oceanologica Acta*, 16(1), 33–43, 1992.

Teruzzi, A., Cossarini, G., Lazzari, P., Salon, S., & Solidoro, C.: Anomalous 2022 deep-water formation and intense phytoplankton bloom in the Cretan area. *Ocean Science Reports*, 4, OSR8, <https://doi.org/10.5194/osr-4-15-2024>, 2024.

Theocharis, A., Georgopoulos, D., Lascaratos, A., Nittis, K.: Water masses and circulation in the central region of the Eastern Mediterranean: Eastern Ionian, South Aegean and Northwest Levantine, 1986–1987. *Deep Sea Research Part II: Topical Studies in Oceanography* 40 (6), 1121–1142, [http://dx.doi.org/10.1016/0967-0645\(93\)90064-T](http://dx.doi.org/10.1016/0967-0645(93)90064-T), 1993.

Theocharis, A., Balopoulos, E., Kioroglou, K., Kontoyiannis, H., Iona, A.: A synthesis of the circulation and hydrography of the South Aegean Sea and the Straits of the Cretan Arc (March 1994–January 1995). *Progress in Oceanography* 44 (4), 469–509. [http://dx.doi.org/10.1016/S0079-6611\(99\)00041-5](http://dx.doi.org/10.1016/S0079-6611(99)00041-5), 1999a.

Theocharis, A., Nittis, K., Kontoyiannis, H., Papageorgiou, E., Balopoulos, S.: Climatic changes in the Aegean Sea influence the Eastern Mediterranean thermohaline circulation (1986 – 1997), *Geophys. Res. Lett.*, 26 (11), pp.1617 – 1620, <http://dx.doi.org/10.1029/1999GL900320>, 1999b.

Theocharis, A., Klein, B., Nittis, K., Roether, W.: Evolution and status of the Eastern Mediterranean Transient (1997–1999), *Journal of Marine Systems*, 33–34, pp. 91-116, [http://dx.doi.org/10.1016/S0924-7963\(02\)00054-4](http://dx.doi.org/10.1016/S0924-7963(02)00054-4), 2002.

Theocharis, A., Krokos, G., Velaoras, D. and Korres, G.: An Internal Mechanism Driving the Alternation of the Eastern Mediterranean Dense/Deep Water Sources. In *The Mediterranean Sea* (eds G.L.E. Borzelli, M. Gačić, P. Lionello and P. Malanotte-Rizzoli), <https://doi.org/10.1002/9781118847572.ch8>, 2014.

Velaoras, D., Krokos, G., Nittis, K., and Theocharis, A.: Dense intermediate water outflow from the Cretan Sea: A salinity driven, recurrent phenomenon, connected to thermohaline circulation changes, *J. Geophys. Res. Oceans*, 119, 4797– 4820, <http://dx.doi.org/10.1002/2014JC009937>, 2014.

Velaoras, D., Krokos G., and Theocharis A.: Recurrent intrusions of transitional waters of Eastern Mediterranean origin in the Cretan Sea as a tracer of Aegean Sea dense water formation events, *Progr. Oceanog.*, Vol. 135, 113–124, <https://doi.org/10.1016/j.pocean.2015.04.010>, 2015.



640 Velaoras, D., Papadopoulos, V., Kontoyiannis, H., Cardin, V., and Civitarese, G.: Water masses and hydrography during April  
and June 2016 in the Cretan Sea and Cretan passage (Eastern Mediterranean Sea), Deep Sea Res. Part II Top. Stud. Oceanogr.  
164, 25–40, <https://doi.org/10.1016/j.dsr2.2018.09.005>, 2019.

Velaoras, D., Zervakis, V., Theocharis, A.: The Physical Characteristics and Dynamics of the Aegean Water Masses. In:  
Anagnostou, C.L., Kostianoy, A.G., Mariolakos, I.D., Panayotidis, P., Soilemezidou, M., Tsaltas, G. (eds) The Aegean Sea  
645 Environment. The Handbook of Environmental Chemistry, vol 127. Springer, Cham. [https://doi.org/10.1007/698\\_2020\\_730](https://doi.org/10.1007/698_2020_730),  
2021.

Velaoras, D., Kioroglou, S., Bourma, E., Ballas, D., and Zervakis, V.: Evidence of thermohaline staircase in the Cretan Sea  
(Eastern Mediterranean Sea). *Front. Mar. Sci.* 12:1649311, <https://doi.org/10.3389/fmars.2025.1649311>, 2025.

Vervatis, V., Sofianos, S., and Theocharis, A.: Water mass distribution and formation processes in the Aegean Sea, *Geophys.*  
650 *Res. Abstr.*, 11, EGU 2009-4794, <http://meetings.copernicus.org/egu2009>, 2009.